Available online at www.sciencedirect.com

ScienceDirect

Nuclear Data Sheets 120 (2014) 211–214

Nuclear Data Sheets

www.elsevier.com/locate/nds

The FLUKA Code: Developments and Challenges for High Energy and Medical Applications

T.T. Böhlen,[1] F. Cerutti,[1] M.P.W. Chin,[1] A. Fassò,[2] A. Ferrari,[1,*] P.G. Ortega,[1] A. Mairani,[3] P.R. Sala,[4] G. Smirnov,[1] and V. Vlachoudis[1]

[1] *European Laboratory for Particle Physics (CERN), CH-1211 Geneva 23, Switzerland*
[2] *ELI Beamlines, Harfa Office Park Ceskomoravská 2420/15a, 190 93 Prague 9, Czech Republic*
[3] *Unità di Fisica Medica, Fondazione CNAO, I-27100 Pavia, Italy*
[4] *Istituto Nazionale di Fisica Nucleare, Sezione di Milano, Via Celoria 16, I-20133 Milano, Italy*

The FLUKA Monte Carlo code is used extensively at CERN for all beam-machine interactions, radioprotection calculations and facility design of forthcoming projects. Such needs require the code to be consistently reliable over the entire energy range (from MeV to TeV) for all projectiles (full suite of elementary particles and heavy ions). Outside CERN, among various applications worldwide, FLUKA serves as a core tool for the HIT and CNAO hadron-therapy facilities in Europe. Therefore, medical applications further impose stringent requirements in terms of reliability and predictive power, which demands constant refinement of sophisticated nuclear models and continuous code improvement. Some of the latest developments implemented in FLUKA are presented in this paper, with particular emphasis on issues and concerns pertaining to CERN and medical applications.

I. INTRODUCTION

The CERN accelerator complex exploits a unique combination of accelerators. The injector chain produces proton and ion beams ranging from 50 MeV (LINAC2) to 450 GeV/c (SPS). The flagship accelerator, the LHC, has already accelerated and collided proton beams at 4 TeV, and lead ion beams at 1.6 TeV/n, with the planned aim of achieving energies of 7 TeV and 2.7 TeV/n, respectively.

The equivalent laboratory energy range for proton beams at CERN spans from a few MeV up to 10^5 TeV. The FLUKA [1, 2] code is the workhorse behind all beam-accelerator calculations [3], as well as many calculations specific to individual experiments around the accelerator complex. Areas where FLUKA simulations are routinely required at CERN are secondary beam design, energy deposition (quenching, damage), radiation damage (electronics, insulation), shielding activation, residual dose rates, and waste disposal. The code has also been extensively used for calculations of the radiation field in the Earth's atmosphere and in space.

These applications require physics models to be reliable across a wide energy range, covering all elementary particle and ion beams up to uranium. FLUKA is jointly developed by the European Laboratory for Particle Physics (CERN), and the Italian National Institute for Nuclear Physics (INFN). The approach to hadronic interaction modelling in FLUKA has been described in several papers [4, 5]. Hadron-nucleon inelastic collisions are described in terms of resonance production and decay up to a few GeV. At higher energies, a model based on the Dual Parton Model [6] (DPM) takes over. Hadron-nucleus ($h-A$) interactions as modelled in FLUKA can be schematically described as a sequence of the following steps:

- Glauber-Gribov cascade and high-energy collisions,
- Generalized-Intra Nuclear cascade,
- Pre-equilibrium emission,
- Evaporation/Fragmentation/Fission and final de-excitation.

Some of the steps can be omitted by design, depending on the projectile energy and identity. Nucleus-nucleus collisions are treated by three different models depending on the energy range; details of the nuclear models can be found in Ref. [7] and references therein. Some recent developments in FLUKA are presented in this paper.

II. DESIGNING NEUTRINO BEAMS

Conventional neutrino beams, like the CERN Neutrino to Gran Sasso (CNGS) beam [8], are produced with accelerated proton beams in a two-step process. The primary

* Corresponding author: alfredo.ferrari@cern.ch

http://dx.doi.org/10.1016/j.nds.2014.07.049

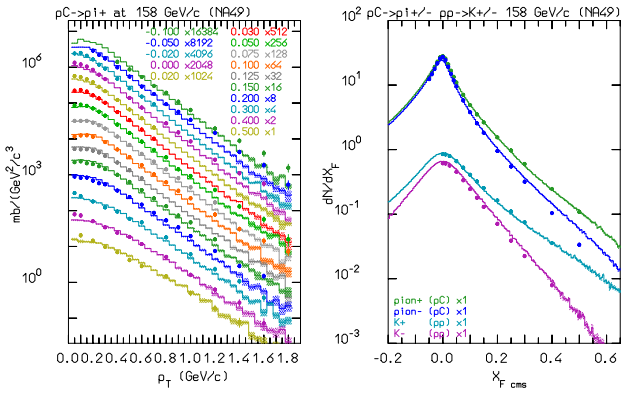

FIG. 1. Left: Double differential π^+ production for 158 GeV/c protons on carbon as a function OF p_T for various X_F values (legend: X_F values and scaling factor among curves). Right: p_T integrated π^+ (green, top) π^- (blue, second from top) production for the same reaction and K^+ (red, second from bottom), K^- (purple, bottom) production for pp at the same energy. Histograms computed by FLUKA ; symbols experimental data from [9, 10]. The dashed areas represent the statistical errors of the calculation.

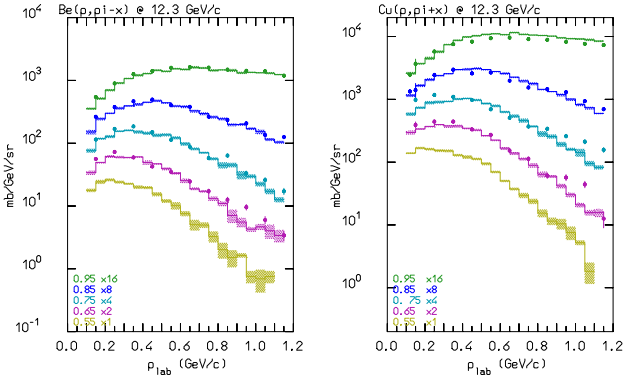

FIG. 2. Pion production (π^- from Be left, π^+ from Cu right) from proton interactions at 12.3 GeV/c. Double differential pion spectra as a function of momentum for different $\cos\theta$ intervals in the range 0.5-1 (legend: $< \cos\theta >$ and scaling factor among curves). Symbols: data (BNL910 expt. [13]), histograms: FLUKA . The dashed areas represent the statistical errors of the calculation.

beam hitting a thick target produces charged mesons (pions and kaons). Mesons are collimated by magnetic lenses into a vacuum or helium pipe where they decay producing neutrinos and associated leptons. The energy spectrum and "polarity" (neutrinos or anti-neutrinos) are defined by the magnetic lenses. The resulting neutrino beam is mainly composed of ν_μ from π and, to a lesser degree, K decay, with a small component (order of a few %) of ν_e from μ and K decay. A precise knowledge of this small contamination is crucial for present and future experiments. For instance, the CNGS beam, produced by 400 GeV/c protons, was designed to produce a high energy ($15-30$ GeV) ν beam in order to detect the oscil-

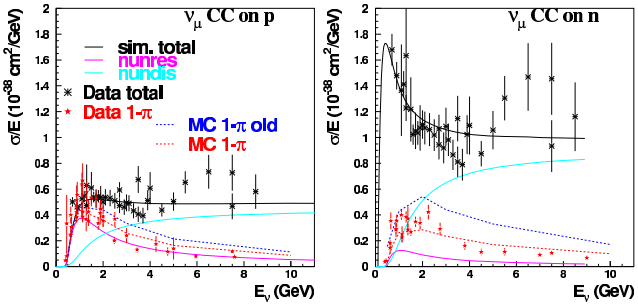

FIG. 3. Cross sections for reactions induced by muon neutrinos on protons (left) and neutrons (right). Data (symbols, from the compilation in [12]) are presented for the total cross section (black) and for the "single π" cross section (red). The total simulated cross section (black line) is composed of the QE (not shown), resonant (magenta line) and DIS (cyan line) channels. The red dotted line shows the calculated "single π" cross section in the present FLUKA version, while the dotted blue line corresponds to the old FLUKA results.

lation $\nu_\mu \to \nu_\tau$ through identification of the $\tau \to e + X$ decay: the expected number of events, before applying powerful selection criteria, is ten times smaller than the ν_e contamination. CERN is now designing a possible neutrino facility (called CENF, with a 100 GeV/c p beam and a low energy, $1-3$ GeV, ν beam) for sterile neutrino detection through $\nu_\mu \to \nu_e$ appearance, where signal and background will be of the same order of magnitude. A near and far detector configuration is envisaged to constrain the uncertainty on the background, nevertheless the simulations need to be highly accurate. The most important source of uncertainties in the ν_μ and ν_e flux predictions is the simulation of meson production in the target. FLUKA is the tool used in the past to design CNGS, and at present to design CENF. The accuracy of this code in describing meson production at proton energies near design for CENF is shown in Fig. 1. Taking into account the focusing system, p_T integrated data are the most representative for judging the accuracy of meson production for neutrino beams. As shown in Fig. 1, right, an agreement with experimental data [9] at the level of a few percent is obtained in the relevant range of Feynman X, both for pion and kaon production. At the other end of the neutrino beam, the knowledge of neutrino cross sections and of the reaction kinematics is another major source of uncertainty. FLUKA has its own neutrino interaction generator, called NUNDIS [11], that embeds the basic neutrino-nucleon interaction in the PEANUT nuclear environment [5]. NUNDIS also borrows the same chain hadronization algorithm used in the hadron-hadron interaction model. Both in neutrino and hadron interactions above a few GeV, (i.e. above the validity of resonance-based models), interactions are modeled as the formation of quark-gluon chains and their subsequent fragmentation into nucleons and mesons. However, standard hadronization is outside its validity region when low mass chains are involved, mainly because of strong mass effects. To

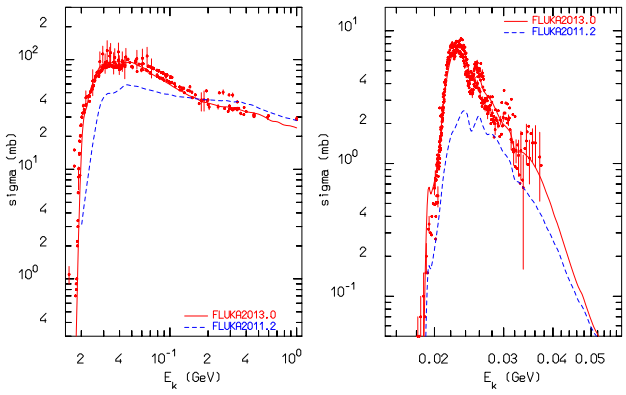

FIG. 4. ^{nat,12}C$(p,x)^{11}$C (left), and ^{nat,12}C$(\gamma,n)^{11}$C (right) cross sections as computed with FLUKA2013.0 (red, upper curve), and FLUKA2011.2 (blue, lower curve) compared with data retrieved from the EXFOR library [16] .

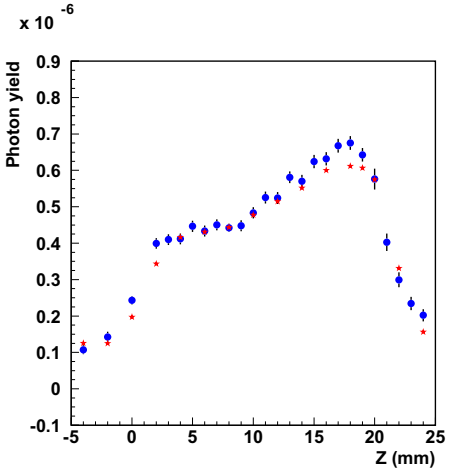

FIG. 5. Prompt photon yield at 90° as a function of depth for a 95 MeV/n ^{12}C beam impinging on a PMMA target. The Bragg peak position is at ≈20 mm. Absolute comparison of data (red stars) [18] (the original experimental data have been re-evaluated in 2012) and FLUKA (blue circles).

better cope with hadron production and neutrino interactions in the few-GeV range, a new treatment of low mass chains has been implemented in FLUKA . These chains gradually migrate from standard hadronization to a phase space explosion analog to the Fermi Break-up of light nuclei. Thus the chain is hadronised in a single step, emitting baryons, mesons and resonances with multiplicity and momenta sampled according to phase space density. Two constraints are enforced through random rejection. First of all, the most energetic particle is preferentially the one carrying a projectile quark. Second, in order to comply with the experimentally observed transverse momentum distributions, configurations where the product of all transverse momenta largely exceeds $N \cdot 0.3$ GeV (N being the number of secondaries) are progressively disfavored. Results of this new approach agree well with thin target experimental data, as shown for instance in Fig. 2.

This new low mass chain treatment has a spectacular impact on the prediction of the "single pion production" reactions in ν induced reactions, such as, for example, $\nu_\mu + p \rightarrow \mu^- + p + \pi^+$. These are the natural outcome of the resonant channel; the above example could come from $\nu_\mu + p \rightarrow \mu^- + \Delta^{++} \rightarrow \mu^- + p + \pi^+$. However, the DIS channel can also result in single pion production. Both processes must be considered when comparing with experimental data. FLUKA results after the latest improvement are in good agreement with data, while they previously overestimated the single pion channels (see Fig. 3).

III. DEVELOPMENTS OF INTEREST FOR HADRONTHERAPY MONITORING

^{16}O(p,x)^{15}O and ^{12}C(p,x)^{11}C are the most important reactions for in-vivo or off-line PET (Positron Emission Tomography) monitoring of proton therapy [15]. They can proceed through emission of either independent nucleons or deuterons. A reliable prediction of these channels is critical, particularly at energies typical of the Bragg peak region for protons. Composite ejectiles like d, t, ^{3}He, and α can be reasonably described by coalescence algorithms during the intranuclear cascade and pre-equilibrium stages. All possible combinations of unbound nucleons and/or light fragments are checked at each stage of system evolution and a figure-of-merit evaluation based on phase space closeness at the nucleus periphery is used to decide whether a light fragment is formed. This approach works reasonably well at medium/high energies; and has been recently extended up to intermediate mass fragments of mass $A \leq 10$ [14]. However, at energies below a few tens of MeV, coalescence is increasingly ineffective in reproducing the data. Recently, a direct deuteron formation mechanism following the first pn or np elementary interaction has been implemented in FLUKA which greatly improved the predictive power for reactions such as (p,d). An example outlining the effectiveness of the new approach and directly relevant for proton therapy monitoring with PET is given in Fig. 4(left).

Another promising technique for in-vivo hadrontherapy monitoring relies on the detection of prompt photons emitted following nuclear interactions by the beam particles. FLUKA capabilities in this aspect have been recently enhanced [17], and an example is given in Fig. 5.

IV. SPIN AND PARITY EFFECTS

Statistical evaporation of excited low mass fragments is unsuitable due to the relatively few, widely spaced levels. Therefore, alternative de-excitation mechanisms are employed for these light (typically A≤16) residual nuclei in most Monte Carlo (MC) codes. A popular choice for

these calculations is the Fermi Break-up model [19, 20], where the excited nucleus is supposed to disassemble in one single step into two or more fragments, possibly in excited states, with branching given by plain phase space considerations. In particular, the probability for breaking-up a nucleus of N neutrons, Z protons, and U excitation energy (total mass $M^* = U + M_{A,Z}$) into n fragments ($n \geq 2$) of the same total charge and baryon number, is given by

$$W = \frac{S_n}{G}\left[\frac{V_{\rm br}}{(2\pi\hbar)^3}\right]^{n-1}\left(\frac{1}{M^*}\prod_{i=1}^{n} m_i\right)^{3/2} \frac{(2\pi)^{3(n-1)/2}}{\Gamma(\frac{3}{2}(n-1))}E_{\rm kin}^{3n/2-5/2}, \quad (1)$$

where the spin factor S_n, and the permutation factor G are given by (n_j is the number of identical particles of jth kind)

$$S_n = \prod_{i=1}^{n}(2S_i+1), \qquad G = \prod_{j=1}^{k} n_j!, \quad (2)$$

and $E_{\rm kin}$ is the total kinetic energy of all fragments at the moment of break-up given by

$$E_{\rm kin} = M^* - \sum_{i=1}^{n} m_i - E_{Coul}, \quad (3)$$

where E_{Coul} is the Coulomb energy in case there is more than one charged particle. $V_{\rm br}$ is a volume of the order of the initial residual nucleus volume. Therefore, the final state can be conveniently selected by means of a MC procedure, through evaluating such an expression for all combinations of fragments energetically allowed and making a random selection. However, Eq. 1 implicitly assumes that the fragment emission occurs in L=0 and neglects consideration of the initial spin and parity state, J^π, of the excited nucleus. If the initial J^π is known, suitable modifications must be applied to Eq. 1 in order to account for the spin and parity, in particular:

- The minimum orbital momentum L_{min} compatible with J^π and the spins and parities of the emitted particles must be computed.
- The spin factor S_n must be restricted to the spin projections compatible with an emission with L_{min}.
- In case $\mathrm{L}_{min} > 0$, a suitable centrifugal barrier must be added to E_{Coul}.

An example of the improvement arising from the inclusion of spin/parity considerations is presented in Fig. 4, right, where the calculated excitation curve for $^{12}\mathrm{C}(\gamma,n)^{11}\mathrm{C}$, a reaction for which $J^\pi = 0^+$ in the GDR energy range is compared with experimental data before and after their application. This reaction is of special relevance for underground experiments, particularly those using liquid scintillators, where photons produced by high energy muons penetrating through the underground rock can produce ^{11}C and neutron background.

V. CONCLUSIONS

The FLUKA code is used for a variety of applications at CERN and elsewhere. Some of the recent improvements of relevance for CERN problems, mostly ν beams and interactions, underground experiments, and medical applications have been described, together with examples showing the improved results when compared with experimental data.

Acknowledgements: This project was partially supported by ENVISION, which is co-funded by the European Commission under FP7 Gr. Agreement N. 241851.

[1] A. Ferrari, P.R. Sala, A. Fassò, J. Ranft, FLUKA: A MULTI-PARTICLE TRANSPORT CODE, CERN-2005-10, INFN/TC_05/11, SLAC-R-773 (2005).
[2] G. Battistoni *et al.*, AIP CONF. PROC. **896**, 31, (2007).
[3] V. Boccone *et al.*, NUCL. DATA SHEETS **120**, 215 (2014).
[4] A. Ferrari, and P.R. Sala, PROC. WORKSHOP ON NUCLEAR REACTION DATA AND NUCLEAR REACTORS PHYSICS, DESIGN AND SAFETY, A. Gandini, G. Reffo eds., **2**, 424 (1998).
[5] G. Battistoni *at al.*, PROC. 11TH INTERNATIONAL CONFERENCE ON NUCLEAR REACTION MECHANISMS, E. Gadioli ed., 483 (2006).
[6] A. Capella, U. Sukhatme, C.-I. Tan, J. Tran Thanh Van, PHYS. REP. **236**, 225 (1994).
[7] F. Ballarini *et al.*, ADV. SPACE RAD. **40**, 1339 (2007).
[8] D. Autiero *et al.*, NUCL. PHYS. B, PROC. SUPPL. **189**, 263 (2009).
[9] C. Alt *et al.*, EUR. PHYS. J. C **49**, 897 (2007).
[10] T. Anticic *et al.*, EUR. PHYS. J. C **68**, 1 (2010).
[11] G. Battistoni *et al.*, AIP CONF. PROC. **1189**, 343 (2009).
[12] J. Beringer *et al.*, PHYS. REV. D **86**, 010001 (2012).
[13] I. Chemakin *et al.*, PHYS. REV. C **65**, 024904 (2002).
[14] A. Boudard *et al.*, PHYS. REV. C **87**, 014606 (2013).
[15] K. Parodi, A. Ferrari, F. Sommerer, H. Paganetti, PHYS. MED. BIOL. **52**, 3369 (2007).
[16] `http:www-nds.iaea.org/exfor/`
[17] G. Battistoni *et al.*, MODELING PROMPT PHOTON EMISSION WITH FLUKA, *to be published*
[18] F. Le Foulher *et al.*, IEEE TRANS. NUCL. SCI. **57** 2768 (2010).
[19] E. Fermi, PROG. THEOR. PHYS. **5**, 1570 (1950).
[20] M. Epherre, E. Gradsztajn, J. PHYS. **18**, 48 (1967).